Published in final edited form as:
Neuron. 2014 October 1; 84(1): 202–213. doi:10.1016/j.neuron.2014.08.037.

Visual Cortex Modulates the Magnitude but Not the Selectivity of Looming-Evoked Responses in the Superior Colliculus of Awake Mice

Xinyu Zhao[1,2,*], **Mingna Liu**[1,*], and **Jianhua Cang**[1]

[1]Department of Neurobiology, Northwestern University, Evanston, Illinois 60208

[2]Interdepartmental Neuroscience Program, Northwestern University, Evanston, Illinois 60208

Summary

Neural circuits in the brain often receive inputs from multiple sources, such as the bottom-up input from early processing stages and the top-down input from higher-order areas. Here, we study the function of top-down input in the mouse Superior Colliculus (SC), which receives convergent inputs from the retina and visual cortex. Neurons in the superficial SC display robust responses and speed tuning to looming stimuli that mimic approaching objects. The looming-evoked responses are reduced by almost half when the visual cortex is optogenetically silenced in awake, but not in anesthetized mice. Silencing the cortex does not change the looming speed tuning of SC neurons, or the response time course except at the lowest tested speed. Furthermore, the regulation of SC responses by the corticotectal input is organized retinotopically. This effect we revealed may thus provide a potential substrate for the cortex, an evolutionarily new structure, to modulate SC-mediated visual behaviors.

Introduction

A common architecture of sensory circuits is the convergence of bottom-up input from early processing stages and top-down input from various ‘high-order’ brain structures, including higher sensory areas, associative areas and the motor system (Knudsen, 2007). Although studies in many sensory systems have illustrated how cells’ receptive fields are constructed through the bottom-up input, the function of the top-down signal is still poorly understood.

The superior colliculus (SC) (or optic tectum, OT, in lower vertebrates) is an important subcortical structure for sensorimotor integration and provides a great opportunity to address this question. The SC/OT is an evolutionarily conserved structure that receives direct retinal input in all known taxa of vertebrates, even in non-vertebrate chordates (Kusunoki and

Correspondence and requests for materials should be addressed to Jianhua Cang, cang@northwestern.edu, 1-847-467-0478.
*These authors contributed equally to this work.

Amemiya, 1983). It was the most sophisticated visual center until the neocortex recently emerged in mammals. The visual cortex, an evolutionarily new structure, not only implements novel computations on its own, but also influences the old center, the SC, via extensive corticotectal projections (Wang and Burkhalter, 2013). As a result, the SC's visual response is determined by the convergence of the bottom-up retinal input and the top-down cortical input.

The response properties of SC cells are crucial in determining how animals respond to visual stimuli behaviorally. Responses evoked by stimuli of certain features, such as those indicating events of 'interests' or 'emergencies', are further transmitted to the motor command center (e.g. deep SC), allowing the animal to act accordingly (Dean et al., 1989). In order to understand how the SC directs visually-guided behaviors, it is necessary to study how cortical inputs regulate SC cell's responses. Perhaps more interestingly, understanding the function of the cortical input would shed light on how animals could adjust their reactions to visual cues based on their attention state and prior experience. This is because while the retina bears largely hardwired circuits that stably transmit visual information, the cortex is more plastic and subject to profound regulation by the animal's internal state (Ayaz et al., 2013; Niell and Stryker, 2010; Xu et al., 2013). The top-down cortical input to the SC may thus provide a potential neural substrate for voluntary modulation of innate visual behaviors.

To reveal the function of the cortical input to the SC, we have used optogenetic tools in mice to achieve acute and reversible silencing of the visual cortex by activating cortical inhibitory neurons, and determined its effect in both awake and anesthetized conditions. Instead of focusing on orientation/direction selectivity as in almost all previous studies on corticotectal function, we examined SC responses to a looming stimulus because of its clear behavioral relevance. The looming stimulus, which mimics approaching objects, has been widely used in investigating collision detection (Liu et al., 2011; Wu et al., 2005) and target selection in the SC (Mysore et al., 2010, 2011). The ability to detect naturally occurring looming stimulus, likely from approaching predators, is essential for the animal's survival. While rodents rely more on non-visual sensory modalities (e.g. olfactory/somatosensory) for navigating and foraging, vision is believed to be indispensable for quick detection of avian predators (Wallace et al., 2013). Indeed, a recent study showed that the looming stimulus is able to induce a rapid defensive behavior in mice (Yilmaz and Meister, 2013). Our study thus provides a basis for future studies on how visual cortex may regulate behaviors through its modulation of the SC.

Results

Response properties of SC neurons to looming

We first characterized how superficial SC neurons respond to the looming stimulus. Extracellular recordings were made within 400μm below the SC surface, corresponding to the superficial layers of the SC (including both SGS and SO), as confirmed by current source density analysis in a subset of experiments (Supplemental Figure 1; and see Experimental Procedures for details). Thirty eight single units were recorded under urethane anesthesia (n = 13 mice), and 31 units from awake mice (n = 12 mice). In each recording,

the cell's receptive field was first mapped with small squares flashed on the stimulus monitor (Figure 1A). A black circle was then presented at the receptive field center (Figure 1B), with its diameter increasing from 0° to 40° at 6 different speeds (5 to 160°/s in a logarithmic scale). The looming stimuli effectively evoked transient responses in the SC neurons (Figure 1C). The evoked responses increased with the looming speed and saturated gradually in both anesthetized and awake animals (Figure 2A and 2B). Consistently, under both conditions, the majority of SC cells preferred the high speeds of 40–160°/s (84.2% and 100% for the mean response in anesthetized and awake animals, respectively; 63.2% and 83.9% for the peak response; Figure 2C and 2D), with the trend more prominent in awake animals ($p=0.06$ between awake and anesthetized mice, for distributions in Figure 2D, χ^2 test). The most dramatic difference between the two states was the response magnitude, which was significantly higher in awake mice (Figure 2A–B).

Cortical input increases response magnitude in the SC of awake mice without changing selectivity for looming speed

We next investigated the impact of cortical input on the SC responses to the looming stimuli. For this, we used an optogenetic method to silence the visual cortex. Channelrhodopsin-2 (ChR2) was expressed in parvalbumin-positive interneurons in the visual cortex through viral transfection (~200nL of AAV2/1.CAGGS.flex.ChR2. tdTomato.SV40 from University of Pennsylvania vector core). The infected area spanned ~1.8mm in diameter, covering the entire V1 and some of the immediately neighboring higher visual areas (Supplemental Figure 2A). We delivered trains of high intensity blue light pulses by an LED through an optic fiber to the exposed visual cortex, in order to suppress the spiking activity of cortical principal cells (Lien and Scanziani, 2013; O'Connor et al., 2013). We recorded directly from the layer 5 of V1 (Supplemental Figure 3A and 3B), which projects to the SC, and found that the photostimulation nearly completely silenced all the spiking activities (Supplemental Figure 3C and 3D). Even in the higher visual area that was not directly covered by viral expression, the visually-evoked responses were also greatly reduced by optogenetic stimulation, likely due to the elimination of their V1 input (Supplemental Figure 2B and 2C). Since both V1 and higher visual areas project to the SC (Wang and Burkhalter, 2013), the observed effect from this set of experiments (below) is thus likely due to silencing/suppressing all the visual cortical areas.

We first recorded superficial SC cells in anesthetized mice before and after silencing the cortex. Surprisingly, under the anesthetized condition, SC cells' responses to the looming stimuli remained completely unaltered in the absence of cortical input (Figure 3A–C). However, when the same manipulation was performed in awake mice (awake condition was used from here on, unless otherwise stated), a dramatic reduction in SC responses was observed (Figure 3D–F, and Supplemental Figure 4). Silencing visual cortex reduced the SC response magnitude by almost half for all tested looming speeds. Interestingly, the relationship between the response amplitudes under the two conditions was nearly linear, with a slope of 0.54 (Figure 3E and 3F, insets), indicating a role of the cortical input in modulating the gain of looming-evoked SC responses in awake mice. Importantly, SC responses and spontaneous firing rate did not change in the "sham-injected" animals expressing only a fluorescence marker but not ChR2 (Supplemental Figure 5), confirming

that the observed effect was not caused by any non-specific effect of LED illumination. Consistent with the proportional change in SC response magnitude, silencing the cortex did not change the preferred looming speed of individual SC cells (Figure 4A–B). We also calculated the spontaneous firing rate of the SC cells and found a trend of slight reduction when visual cortex was optogenetically silenced, but the difference was not statistically significant ($p = 0.21$; Figure 4C).

It was previously reported in birds and cats that the time course of the responses to looming stimuli is critical for the detection of approaching objects (Liu et al., 2011; Wu et al., 2005). We thus investigated whether silencing cortical input would affect the temporal profile of SC responses. As illustrated by the averaged instantaneous spiking rates (Figure 4D), the response time course remained unchanged after silencing cortex for every looming speed except the slowest one (5°/s), where the activity at ~2–4s after the stimulus onset was more affected by silencing the cortex than the early peak response that occurred at ~350ms.

Taken together, our results reveal that the cortical input modulates the gain of looming-evoked responses in the SC, but does not change its temporal profile or speed tuning. The fact that silencing cortex had no effect on SC responses in anesthetized mice is consistent with the result that SC responses are weaker under this condition (Figure 2A–B).

V1 response properties to looming stimuli

Two possibilities could potentially explain the finding that the looming speed tuning of SC cells is maintained after removing cortical input. First, cortical cells might share the same tuning profile as the SC cells, so that the removal of the same fraction of input at each looming speed would leave the tuning curve unchanged in shape. In other words, the interaction between retinal and cortical inputs would be additive. Alternatively, cortical cells might respond uniformly to different looming speeds and their inputs multiply with retinal inputs, so that the speed-selective component of the SC responses is completely determined by the feedforward input from the retina. In order to distinguish these two scenarios, we studied responses of V1 cells to looming stimuli in awake mice. Infragranular layers (layer 5 and 6) were first identified by current source density analysis (Supplementary Figure 3A and 3B). Single units were recorded within the first 150μm of the infragranular layers, presumably layer 5, where corticotectal cells are located. These V1 cells displayed modest speed-dependent modulation in their responses (Figure 5A–C), with the mean responses doubled across the range of the tested looming speeds, from ~4 spikes/sec for 5°/s to ~8 for 160°/s. This 2 fold change was much smaller compared to the SC tuning, which ranged from ~4 spikes/sec to ~34 spikes/sec, a more than 8 fold increase (compare Figure 5B and Figure 2A).

The observed speed tuning of V1 cells, which is not constant across different speeds, but also not to the same degree of SC cells' tuning, indicates that the interaction between cortical and retinal inputs is not simply additive or multiplicative, but likely a mixture of the two. The interaction between cortical and retinal inputs within the SC circuits likely involves extensive non-linear processing, such as shunting inhibition, short-term plasticity and dendritic spikes. Importantly, our functional analysis showed that the net effect of cortical input on looming-evoked SC response is a linear gain control: the SC responses to

the same visual stimuli are scaled up when cortical input is intact, proportionally across the whole set of looming speed (Figure 3E and F).

The weak looming speed selectivity for cortical responses at the population level could be due to poorly tuned individual cells, and/or diverse speed preferences, so that the individual biases would be averaged out across population. We thus quantified the speed tuning of individual cells using a speed selectivity ratio (SSR, see Experimental Procedures for details). V1 cells showed a significantly smaller SSR than the SC cells (Figure 5D), indicating that individual V1 cells were lesser tuned. In addition, the preferred speed of V1 cells also had a broader distribution than the SC cells (compare Figure 5E with red bars in Figure 2D). In other words, both factors contribute to the relatively poor tuning of cortical responses to looming speed seen at the population level.

We next investigated the time course of V1 responses, and compared it with that of the SC after silencing cortex, which should largely reflect the function of the feedforward input (referred to as SC_{FF} thereafter). V1 response was slower than the SC_{FF}, with the difference more dramatic at the slower looming speeds (Figure 5F). The latency to the peak responses of V1 cells was approximately in proportion to the inverse of the looming speed (Figure 5G). This linear relationship, with a slope of 12.6, means that V1 responses always reached the peak when the diameter of the stimulus expanded to ~13°, regardless of the looming speed. In striking contrast, the peak latencies of SC_{FF} were much more consistent at different looming speeds (Figure 5G), with its peak latency only about doubled when the stimulus was 32-fold slower. As a result, the maximum cortical input comes to the SC significantly later than the retinal input at slow looming speeds, which is in agreement with our observation that the cortical input boosted the late phase of the SC response more than the early peak when the speed was 5°/s (Figure 4D). It should be noted that although cortical responses reached the peak later than the SC_{FF}, their onsets were not apparently different within the resolution of our analysis (Figure 5F). Thus the cortical input could still significantly contribute to the SC's response in the early phase. It remains unclear why cortical input did not facilitate the late phase SC responses more than the early phase at the intermediate speeds (10–80°/s), even though cortical responses were slower in reaching their peaks than SC_{FF}. Non-linear cellular processing as discussed above may be at play as well. For example, surround inhibition is likely recruited during the late phase of looming stimuli, which would make cortical impact relatively smaller when cortical responses are at their peaks. This effect would thus lead to a more uniform postsynaptic cortical impact across the entire response time course.

We then sought to understand why removing cortical input had no effect on SC responses in anesthetized mice. One straightforward explanation is that cortical response to the looming stimuli becomes very weak under anesthesia. Indeed, recordings from V1 layer 5 cells in anesthetized mice showed that their responses were ~50% smaller than in awake conditions (Figure 5B and 5C). Although it is unclear why the remaining cortical activity did not contribute to the visual responses in the SC, our results emphasize the importance of using awake preparations to study the function of the corticotectal pathway.

Cortical influence on SC responses is retinotopically organized

The corticotectal projections are topographically organized to align the retinotopic maps in V1 and the SC (Triplett et al., 2009). We thus tested whether the effect of cortical input on looming-evoked SC responses was also specific to retinotopy. We first performed optical imaging of intrinsic signals to reveal the retinotopic maps in the visual cortex, and guided viral injections to the specified location in V1 that responded to the center of visual stimulus monitor (Figure 6A). Only ~10nL cre-dependent ChR2 virus was injected, which infected a ~450μm diameter area within V1 (Figure 6B), corresponding to 20–30° of visual space (Cang et al., 2005).

We then recorded superficial SC cells in response to the looming stimuli in these injected mice under awake condition as described before. SC cells that had receptive fields near the center of the stimulus monitor, i.e., the region represented by the infected area in V1, showed significant reduction of visual responses after the small area of V1 was silenced optogenetically (Figure 6C–D). In contrast, the SC cells with receptive fields away from the monitor's center were not affected (Figure 6C and E). In fact, the extent of response reduction, quantified by the transformation slope for each individual SC cell, significantly correlated with the distance between the cell's receptive field center and the center of the monitor (Figure 6F). These data thus indicate that corticotectal inputs boost the gain of looming-evoked SC responses in a retinotopic manner: the modulation of SC responses by V1 is restricted to SC neurons that have corresponding receptive fields in visual space.

Discussion

By recording looming-evoked responses in the SC before and after silencing the visual cortex, we have revealed a gain control mechanism by the corticotectal input. The cortical input increases the looming-evoked SC responses across all speeds, while leaving the speed tuning and temporal dynamics unaltered. Furthermore, this effect is retinotopically organized and only present in awake, but not in anesthetized mice. Our study thus reveals how an evolutionarily new structure (the visual cortex) interacts with an old visual center (superior colliculus) in response to a behaviorally relevant visual stimulus.

Comparison with previous studies

A number of studies have investigated the impact of cortical input on the SC's direction selectivity in mice (Wang et al., 2010), cats (Hoffmann and Straschill, 1971; Ogasawara et al., 1984; Rizzolatti et al., 1970; Rosenquist and Palmer, 1971; Wickelgren and Sterling, 1969) and monkeys (Schiller et al., 1974). Unfortunately, these studies led to contradictory conclusions. For example, the effect of cortical input on the superficial SC's responsiveness has been reported to be facilitatory (Ogasawara et al., 1984; Wickelgren and Sterling, 1969), suppressive (Hoffmann and Straschill, 1971) or insignificant (Schiller et al., 1974; Wang et al., 2010). Response selectivity of SC cells has been reported to be either dependent (Ogasawara et al., 1984; Rosenquist and Palmer, 1971; Wickelgren and Sterling, 1969) or largely independent (Hoffmann and Straschill, 1971; Schiller et al., 1974; Wang et al., 2010) on cortical input. Although our results cannot be directly compared with these studies

because of the difference in visual stimuli (looming vs. moving dots/bars/gratings), our study highlights two technical issues that are important in resolving these discrepancies.

First, it is critical to manipulate cortical inputs acutely in order to track changes within individual SC cells and to avoid complications from plasticity. The first issue is especially important because SC cells have diverse response magnitudes and tuning properties. Cortical ablation was used in the majority of previous studies, and the resulting mechanical disturbance and required surgical time made it difficult to keep recording the same cells before and after the manipulation. Although cooling was attempted in a few studies to silence cortex acutely, these experiments themselves also reached conflicting conclusions (Hoffmann and Straschill, 1971; Ogasawara et al., 1984; Schiller et al., 1974), probably due to the poor control of the area and extent of cooling. In our study, we took advantage of optogenetic tools in mice and demonstrated that interneuron photoactivation is an effective and reversible approach to silence cortex and has good spatial and temporal control. Some of the previous experiments regarding direction selectivity could now be repeated with this new silencing method in mice and other species where genetic tools are available.

A second issue is the wakefulness of the animal. Most early experiments were done under anesthetized conditions. The potential influence of anesthesia was proposed but never tested thoroughly (Hoffmann and Straschill, 1971). Here, we performed our experiments in both awake and anesthetized mice, keeping all manipulation and stimulus protocols the same. Our results clearly showed that the substantial contribution of cortical input on the SC could be completely masked by anesthesia. This dramatic difference between anesthetized and awake conditions may explain some of conflicting results in previous studies, and more importantly, should be noted by future studies that aim to investigate the corticotectal pathway. The reason why cortical regulation of SC responses is absent in anesthetized mice is not fully understood. Our results reveal that the low responsiveness of cortical cells under anesthesia is at least one of the factors. Corticotectal synapses may have non-linear properties, such as short-term facilitation and/or large component of NMDAR-mediated currents. If so, the spiking responses of cortical cells under anesthesia, although not absent, may be too low to elicit any detectable postsynaptic effect. Similar non-linear properties are well documented for the corticothalamic synapse, which is classified as ‘modulator’ but not ‘driver’ (Sherman, 2012). Additionally, the urethane anesthesia we used could specifically affect certain channels preferentially located at cortical but not retinal synapses.

Modulation of SC responses by corticotectal input

Our results indicate that cortical input does not determine the selectivity of SC cells for looming speed, but just increases their response magnitude. This observation provides insights on how sensory-guided innate behaviors could be modulated by attention and learning. The sensory layer of the SC functions as a saliency filter. An animal living in its natural environment is always exposed to multiple streams of sensory information simultaneously. The strongest stimulus, indicating the highest priority (e.g. the fastest approaching object), would pop out through competition in the SC, and in turn guide the animal’s behavior accordingly (Knudsen, 2007). Top-down signals from the cortex elevates the responsiveness, but does not change this ‘priority rank’. In certain behavioral context,

the cortical input may highlight a specific location, or weigh one sensory modality over the others. However, stimuli within the 'interest regime' would still compete with each other in a fixed manner, ensuring proper target selection.

Most previous studies on top-down control have focused on associative areas. For example, the input from arcopallial gaze field (AGF), a bird forebrain gaze control area, was shown to modulate the gain of visual and auditory responses in barn owl's tectum (Winkowski and Knudsen, 2007, 2008). However, even earlier processing stages may also be important sources for top-down control. Increasing evidence has started to reveal behavior state dependent modulations in primary sensory cortices, including V1 (Ayaz et al., 2013; Niell and Stryker, 2010), probably because these primary areas themselves are subject to top-down control by high-order areas and/or the motor system. Our results show that visual cortical input approximately doubles visual responses of SC cells. Given such a huge effect, behavioral modulation of cortical activity is expected to have a significant impact on the SC's responsiveness. Recent efforts of mapping brain connectivity in mice begin to reveal a very complex projections pattern to the SC from various cortical areas, including primary and higher visual cortex, other sensory, motor, cingulate and frontal cortices (Oh et al., 2014). Interestingly, only V1 and some higher visual areas targets superficial layers of the colliculus, with all other cortical cells projecting to intermediate and/or deep layers. Among the superficial SC projecting areas, V1 has much higher projection density than others (Wang and Burkhalter, 2013). Therefore V1 might be specifically important for behavior-state dependent modulation of superficial SC. Furthermore, since the deep layers of the SC also receive inputs from the superficial layers, it is of great interest for future studies to understand how the SC integrates cortical signals at different processing stages.

The function of cortical inputs in shaping SC responses largely depends on how cortical cells respond to the visual stimuli in question. This was why we characterized the response properties of V1 layer 5 cells to the looming stimuli. Layer 5 contains a diverse group of pyramidal cells projecting to different brain areas. Targeted recording from the corticotectal projecting cells in future studies is necessary for determining whether this subpopulation has any specific properties. Nonetheless, the fact that the impact of silencing cortex on the SC's responses to looming stimuli can be largely explained by the response properties of the layer 5 cells in our recordings suggests that the recorded layer 5 cells might be representative for the corticotectal cells.

It should be noted that although we found a ~50% reduction in spiking responses of SC cells after silencing cortex, it is likely that the cortical input is still weaker than the retinal input because we recorded postsynaptic spiking rate but not synaptic currents. It requires a substantial membrane potential depolarization of postsynaptic SC cells to reach the spiking threshold. The retinal input alone can effectively drive SC cells to fire, while the cortical input further increases the spiking rate. Together, as shown in several other systems (e.g. retinal and cortical projections to lateral geniculate nucleus), the feedforward input is the primary driver and determinant of the cell's selectivity, while other inputs modulate the response magnitude.

Response to looming in the mouse superior colliculus

We have tested looming stimuli from a very low speed by which only modest responses were evoked, to a very high speed at which saturating responses were observed. Our results revealed that SC cells, as a population, responded to every speed that we tested (5–160°/s). At the same time, the majority of SC cells responded more vigorously to faster stimuli, resulting in a population response increasing with speed and saturated at 80–160°/s. This result indicates that the mouse SC is able to detect objects approaching with a very large range of speed, while biased to the faster ones (at least up to 160°/s), which likely indicates a more 'urgent' event.

Speed tuning is closely related to the cell's receptive field organization (Mysore et al., 2010). Cells in the SC/OT in all species tested so far share a common 'Mexican-hat' structure in their receptive fields, with a narrow excitatory center and a more dispersed inhibition (Del Bene et al., 2010; Mysore et al., 2010; Schiller and Koerner, 1971; Wang et al., 2010; Wu et al., 2005). Such a structure is important for sharpening spatial resolution and mediating lateral competition among SC cells. However, the surround suppression also constrains the cell's response to fast looming objects, because the stimulus would quickly recruit inhibition, thus reducing the effect of excitation. Actually, the peak spiking rate of SC cells already starts to decline at 160°/s, and is expected to continue to decrease with further increase of speed (flashing of a big circle, which can be mathematically viewed as a looming stimulus with an infinite speed, usually evokes very little response due to the surround suppression). Consistently, a recent study showed that an extremely fast looming stimulus (350°/s) is less effective in inducing rapid defensive behavior in mice than a moderate speed (35°/s) (Yilmaz and Meister, 2013). Therefore, the strength and size of surround suppression must be tuned to the animal's ecological context through evolution, to match the SC's speed sensitivity with the looming signals that are important for the animal's survival, such as the approaching of its natural predators.

Two intriguing differences were observed between the SC and V1 in response to looming stimuli, which may reflect the functional dichotomy of the two visual pathways. First, V1 cells are weakly tuned to speed, not as strongly biased toward the faster stimulus as seen in the SC. Second, the response of V1 cells is dramatically delayed at slower speeds, while SC cells are able to maintain relatively fast responses. This phenomenon, although not quantitatively analyzed, was also evident in several example recordings in barn owls. Such a fast sensory response across a large range of stimulus speeds may be critical for mediating rapid behavioral response (Yilmaz and Meister, 2013). One explanation for the difference of response dynamics between these two structures is that layer 5 V1 cells, which primarily receive intracortical inputs, are about three more synapses away from the retina than SC cells (or 1 more if there is direct thalamic input to V1 layer 5 as in somatosensory cortex (Constantinople and Bruno, 2013). This explanation, however, is unlikely to fully account for the slow cortical response, because the difference of peak latencies between the cortex and SC is ~2s for the looming speed of 5°/s and ~1s for 10°/s, far longer than what is expected from a few synaptic delays. Furthermore, although the peak of cortical responses appeared very late with slow stimuli, the response onset was not apparently delayed. Our hypothesis is that SC receptive fields have a strong excitatory center, so that even the

contrast change within a small area during the initial phase of looming can reliably drive the cell's firing at high rates. The response is then quickly shut down by inhibition, resulting in a fast response peak. In contrast, cortical cells may gradually integrate modest inputs from increasing larger areas within their receptive fields when the stimulus looms, and the response reaches its peak when the stimulus gets to a certain size. The weaker surround suppression, as reported in deep layer cortical cells (Nienborg et al., 2013; Vaiceliunaite et al., 2013), might allow the response to build up during a relatively long period.

EXPERIMENTAL PROCEDURES

Animal Preparation

Adult (postnatal day 60–90) C57BL/6 wild-type and *Pvalb-cre* (Jackson Laboratory, stock #008069) mice were used in all recordings. For characterizing response properties in the SC (Figure 1), data were pooled from untreated wild-type mice and the *Pvalb-cre* mice that had ChR2 expression in their visual cortex (but without LED illumination during recordings). All experimental procedures were approved by Northwestern University Institutional Animal Care and Use Committee.

In anesthetized recordings, mice were first sedated by chlorprothixene (5 mg/kg in water, i.p.) and then anesthetized with urethane (1g/kg in 10% saline solution, i.p.), as described before (Zhao et al., 2013). Atropine (0.3 mg/kg, in 10% saline) and dexamethasone (2 mg/kg, in 10% saline) were administrated subcutaneously. The animal was then transferred onto a heating pad for recording. Its body temperature was monitored through a rectal thermoprobe and maintained at 37°C through a feedback heater control module. Toe-pinch reflex was monitored during experiments as a test for the anesthesia depth. 0.2–0.3g/kg urethane was re-dosed when necessary. For SC recordings, a small craniotomy (~1.5mm×1.5mm) was made with its center at 0.75mm lateral and 0.5mm anterior to the Lambda point. For recording in the visual cortex, the center of the craniotomy was 2.9mm lateral and 0.5mm anterior from the Lambda point. For experiments in which SC recording was combined with cortex silencing, a large craniotomy was made (~3.5mm×1.5mm) to access both the SC and visual cortex. Dura was intact in all recordings.

For awake recordings, a small metal plate was first mounted on the mouse's skull with MetaBond (Parkell) under isoflurane anesthesia as described before (Zhao et al., 2013). The animal was then transferred back to its cage that was placed on a heating pad to prevent hypothermia. On the next day, the animal was again anesthetized with isoflurane (1–4% in O_2), and a craniotomy was made in the same way as described for anesthetized recordings. The animal was allowed to recover in its cage for at least 1h with its exposed brain covered with Kwik-Sil Adhesive (World Precision Instruments). During recordings, mice were held via the metal plate, and their bodies were restricted in a plastic tube (Zhao et al., 2013).

Viral Injection and Photostimulation

Adeno-associated virus carrying Cre-dependent ChR2 (AAV2/1.CAGGS.flex.ChR2. tdTomato.SV40) or tdTomato only (AAV9.CAG.flex.tdTomato.WPRE.bGH) was obtained from the University of Pennsylvania Vector Core. For injection, P30–50 *Pvalb-cre* mice

were anesthetized with isoflurane and mounted on a stereotaxic apparatus. A glass pipette with ~20 μm tip diameter was filled with the viral solution and inserted into V1. In one set of experiments, the injections were made at 2.9mm lateral and 0.5mm anterior from the Lambda point. Two injections were made in each animal at 400 μm and 700 μm below the pia, using Nanoject (Drummond). At each depth, 4 times of ~25nl solutions were injected at a speed of ~23nl/s and 30–60s intervals. In another set of experiments, small amount of virus (4.6nL at each depth) was injected to a specific location in V1 as guided by retinotopic maps obtained by intrinsic imaging (details below). After the last injection was made, we waited ~2min before the pipette was slowly retrieved. The skin was closed with surgical suture and the mouse was then allowed to recover from anesthesia. Recordings were done 3–5 weeks after injections.

To photostimulate ChR2 expressing cells, an optic fiber driven by a blue LED (Doric Lens) was placed ~0.5mm above the exposed cortex. During recordings, the tip of LED fiber was buried in the agarose that was applied to reduce the pulsation of the brain and protect the tissue. To prevent direct photostimulation of eyes by the LED light, the agarose surface was painted with black ink, and a piece of thick black paper was carefully placed around the fiber to ensure no light could be seen from the front and lateral sides. This was further confirmed by results in the sham-injected animals where LED illumination did not affect SC responses. Pulses of blue light at 20Hz (10ms duration for each pulse) were delivered starting from 200ms before the onset of each visual stimulus, throughout the entire stimulus duration. The intensity of LED light was ~140mW/mm^2 at the tip of the optic fiber.

Extracellular Recordings and Visual Stimuli

In anesthetized recordings, single unit activities were recorded by tungsten electrodes (5–10MΩ, FHC). In awake recordings, 16-channel silicon probes (50 μm spacing, NeuroNexus Technologies) were used. Electrical signals were sampled using a System 3 workstation (Tucker Davis Technologies) at 25kHz as described before (Zhao et al., 2013). Electrical signals were filtered between 0.3 and 5 kHz for spikes, and 10 and 300Hz for local field potentials.

Visual Stimuli were generated with Matlab Psychophysics toolbox (Brainard, 1997), and were presented using a CRT monitor (60Hz refresh rate, ~35cd/m^2 mean luminance). The monitor was placed on the side contralateral to the recorded hemisphere. Throughout the study, only the animal's contralateral eye was stimulated, while the ipsilateral eye was covered with an eye shutter.

The electrode was inserted vertically into the brain for SC recordings. For recordings with tungsten electrodes, the electrode was first inserted quickly to 700–900 μm below the pia, and then slowly lowered. Estimation of the SC surface followed our published procedure (Wang et al., 2010). Spiking activities were then carefully searched in response to moving bars. Single units were recorded at 50–400μm below the SC surface (typically 1–1.5 mm below the cortex surface), corresponding to the superficial layers of SC. For recordings with 16-channel silicon probes, the probe was directly inserted into the SC with its tip ~1.6mm below cortex surface. Small adjustment of the probe was sometimes made to increase signal-to-noise level of recorded units, but larger electrode movement for cell searching, like that in

tungsten electrode recordings, was never performed. To identify superficial layers of the SC in these recordings, we did current source density analysis as described in Supplemental Figure 1.

After a single unit was isolated, its receptive field position was first estimated with moving bars at various directions. The receptive field was then mapped more accurately with white squares (5° ×5°, 0.5s ON and 0.5s OFF, on a grey background) flashed at different locations within the estimated area. Typical transient responses were observed at both the onset and offset of the stimulus (Wang et al., 2010). Looming black circles on a grey background (~35 cd/m^2) were then presented at the center of the cell's RF at different looming speeds. The final diameter of looming circles was fixed at 40°. Each stimulus was repeated for 5 trials in a pseudorandom order with 1s interval between each condition. A blank stimulus (grey background) was also included for measuring the spontaneous activity. For current source density analysis (supplemental Figure 1), a full-screen checkerboard (each checker of 12.5 ×12.5) was contrast-reversed at every 1 sec as described in (Niell and Stryker, 2008).

For cortical recordings, the electrode was inserted perpendicularly to the cortex surface (~18 from vertical), and layer 5 cells were recorded at 450–650μm below the pia, further confirmed by current source density analysis (Supplemental Figure 3). Our recorded V1 layer 5 cells had spontaneous spiking rates of 0–5 spikes/s (median: 1.3 spikes/s) in anesthetized mice and 1–24 spikes/s (median: 2.1 spikes/s) in awake mice. These values are similar to previously published studies of anesthetized (Niell and Stryker, 2008) and awake mouse V1 (Ayaz et al., 2013).

Recordings with tungsten electrodes obtained unambiguous single units (typically larger than 500μV peak to peak), occasionally with large electric artifact or two units with very different spike waveforms. OpenSorter (Tucker Davis Technologies) was used to remove the artifact and sort different units, in which spike waveforms were first decomposed into 3 principal components, and then isolated by K-mean algorithm. In recordings with 16-channel probes, in which the signal-to-noise ratio was relatively smaller (spike peak-to-peak amplitude was 200–400μV, while the background was typically ~50μV), single units were sorted by OpenSorter as described above. Clear clustering of spike waveforms was sometimes hard to achieve with this software, primarily due to temporally shifted spike waveforms from the same unit when the spike detection threshold was near the background noise. In these cases, spikes were sorted using a customized program, where spikes were first aligned with their peaks and then clustered. Recordings with no clear clustering even using this method were not included in our analysis. In all recordings, we only included the largest one or two units recorded from our 16-channel probe in each penetration where we were confident in the spike sorting, although spiking activities were normally seen at 3–4 other channels.

Optical imaging of Retinotopic Maps

To guide viral injections by retinotopic maps (Figure 6), optical imaging of intrinsic signals was performed through the intact skull in mice under isoflurane anesthesia (1–1.25% in O_2). The imaged area was covered by agarose and a coverslip that formed an imaging window. The spatial frequency of the drifting bar was 1 cycle/100°, and temporal frequency 1 cycle/8

s. Optical images were acquired at 610 nm using a Dalsa 1M30 CCD camera (Dalsa, Waterloo, Canada) and the Fourier component of the reflectance changes was extracted at the temporal frequency of the stimulus as described previously (Kalatsky and Stryker, 2003). To identify higher visual areas for physiology recordings, the animal was anesthetized by urethane as described for physiology recordings, and a large craniotomy (~3×1.5mm) was done to expose the visual cortex. All other imaging procedures were the same as described above.

Histology

After recordings, mice were overdosed with euthanasia solution (150mg/kg pentobarbital), and perfused with PBS and then 4% paraformaldehyde (PFA) solution. The brain was fixed in 4% PFA overnight. Coronal slices of 150μm thick were cut from the fixed brain, using a vibratome (Series 1000 Sectioning System). Both bright-field and fluorescence images were taken by a Zeiss epifluoresence microscope. Electrode tract labeling was done with 2.5% DiI solution in DMSO as described before (Zhao et al., 2013).

Data Analysis

Visually-evoked responses were obtained by subtracting mean spontaneous spiking rates, recorded at the blank stimulus, from spiking rates during the looming stimuli. Speed tuning was quantified by either the mean spiking rate within the whole stimulus duration or the peak instantaneous response calculated with a bin width of 100ms. In both quantifications, responses from multiple trials to the same stimulus were averaged. For characterizing the shape of speed tuning curves, tuning curves of individual cells were first normalized to their own maximum magnitude, and then averaged across the population. In all figures except for Figure 4, the preferred speed was defined as the speed that evoked the strongest response. To obtain a better comparison of the preferred speeds before and after cortex silencing (Figure 4A–B), we calculated $S_{pref_}$weighted to take the whole tuning curve into account. $S_{pref_}$weighted was the mean of stimulus speeds weighted by the evoked response at each speed: $S_{pref\_}weighted=\Sigma (R*speed)/\Sigma(R)$. Speed sensitivity ratio (SSR) was calculated as an index for how selective individual cells are to different looming speeds. Ratios of $R_{pref}/R_{slowest}$ and $R_{pref}/R_{fastest}$ were first calculated, where R_{pref} was the response at the preferred speed, while $R_{slowest}$ and $R_{fastest}$ were responses at the slowest (5 /sec) and fastest (160 /sec) speed, respectively. SSR was defined as the larger one of the two ratios.

To characterize the temporal profile of looming-evoked responses, instantaneous spiking rates were calculated with a bin of 100ms and averaged across the population. To test whether silencing cortex had specific impact on the late phase of SC cells' responses, we first calculated the ratio of peak responses between the control condition and the condition where the visual cortex was silenced (under both conditions the peak occurred shortly after the stimulus onset). The response of each individual cell when the cortex was silenced was then scaled with this ratio, and this normalized response was compared with the control response at each bin.

Current source density (CSD) analysis was performed to identify layers in the SC and V1. In both cases, CSD was calculated from local field potentials (LFPs), following published methods (Niell and Stryker, 2008):$CSD(x)=(2\times LFP(x)-LFP(x+2)-LFP(x-2))/4$;

where x is the channel number for a given depth, and x+2 indicates 2 channels (100um) below and x−2 for 2 channels above.

All pooled data were presented as mean ± s.e.m. Mann-Whitney test was applied for comparing data from different groups of cells, while t-test was applied for paired comparison. χ^2 test was applied for comparing distributions of discrete data. All analyses were performed in Matlab (MathWorks).

Supplementary Material

Refer to Web version on PubMed Central for supplementary material.

Acknowledgments

We thank Dr. Dan Dombeck and Dr. Tom Bozza for sharing reagents and equipment. This work was supported by US National Institutes of Health (NIH) grant (EY020950) to J.C. and HHMI international student fellowship to X.Z.

References

Ayaz A, Saleem AB, Scholvinck ML, Carandini M. Locomotion controls spatial integration in mouse visual cortex. Curr Biol. 2013; 23:890–894. [PubMed: 23664971]

Brainard DH. The Psychophysics Toolbox. Spat Vis. 1997; 10:433–436. [PubMed: 9176952]

Cang J, Kaneko M, Yamada J, Woods G, Stryker MP, Feldheim DA. Ephrin-as guide the formation of functional maps in the visual cortex. Neuron. 2005; 48:577–589. [PubMed: 16301175]

Constantinople CM, Bruno RM. Deep cortical layers are activated directly by thalamus. Science. 2013; 340:1591–1594. [PubMed: 23812718]

Dean P, Redgrave P, Westby GW. Event or emergency? Two response systems in the mammalian superior colliculus. Trends Neurosci. 1989; 12:137–147. [PubMed: 2470171]

Del Bene F, Wyart C, Robles E, Tran A, Looger L, Scott EK, Isacoff EY, Baier H. Filtering of visual information in the tectum by an identified neural circuit. Science. 2010; 330:669–673. [PubMed: 21030657]

Hoffmann KP, Straschill M. Influences of cortico-tectal and intertectal connections on visual responses in the cat's superior colliculus. Exp Brain Res. 1971; 12:120–131. [PubMed: 5555542]

Kalatsky VA, Stryker MP. New paradigm for optical imaging: temporally encoded maps of intrinsic signal. Neuron. 2003; 38:529–545. [PubMed: 12765606]

Knudsen EI. Fundamental components of attention. Annu Rev Neurosci. 2007; 30:57–78. [PubMed: 17417935]

Kusunoki T, Amemiya F. Retinal projections in the hagfish, Eptatretus burgeri. Brain Res. 1983; 262:295–298. [PubMed: 6839158]

Lien AD, Scanziani M. Tuned thalamic excitation is amplified by visual cortical circuits. Nat Neurosci. 2013; 16:1315–1323. [PubMed: 23933748]

Liu YJ, Wang Q, Li B. Neuronal responses to looming objects in the superior colliculus of the cat. Brain Behav Evol. 2011; 77:193–205. [PubMed: 21546772]

Mysore SP, Asadollahi A, Knudsen EI. Global inhibition and stimulus competition in the owl optic tectum. J Neurosci. 2010; 30:1727–1738. [PubMed: 20130182]

Mysore SP, Asadollahi A, Knudsen EI. Signaling of the strongest stimulus in the owl optic tectum. J Neurosci. 2011; 31:5186–5196. [PubMed: 21471353]

Niell CM, Stryker MP. Highly selective receptive fields in mouse visual cortex. J Neurosci. 2008; 28:7520–7536. [PubMed: 18650330]

Niell CM, Stryker MP. Modulation of visual responses by behavioral state in mouse visual cortex. Neuron. 2010; 65:472–479. [PubMed: 20188652]

Nienborg H, Hasenstaub A, Nauhaus I, Taniguchi H, Huang ZJ, Callaway EM. Contrast dependence and differential contributions from somatostatin- and parvalbumin-expressing neurons to spatial integration in mouse V1. J Neurosci. 2013; 33:11145–11154. [PubMed: 23825418]

O'Connor DH, Hires SA, Guo ZV, Li N, Yu J, Sun QQ, Huber D, Svoboda K. Neural coding during active somatosensation revealed using illusory touch. Nat Neurosci. 2013; 16:958–965. [PubMed: 23727820]

Ogasawara K, McHaffie JG, Stein BE. Two visual corticotectal systems in cat. J Neurophysiol. 1984; 52:1226–1245. [PubMed: 6520633]

Oh SW, Harris JA, Ng L, Winslow B, Cain N, Mihalas S, Wang Q, Lau C, Kuan L, Henry AM, et al. A mesoscale connectome of the mouse brain. Nature. 2014; 508:207–214. [PubMed: 24695228]

Rizzolatti G, Tradardi V, Camarda R. Unit responses to visual stimuli in the cat's superior colliculus after removal of the visual cortex. Brain Res. 1970; 24:336–339. [PubMed: 5490294]

Rosenquist AC, Palmer LA. Visual receptive field properties of cells of the superior colliculus after cortical lesions in the cat. Exp Neurol. 1971; 33:629–652. [PubMed: 5132203]

Schiller PH, Koerner F. Discharge characteristics of single units in superior colliculus of the alert rhesus monkey. J Neurophysiol. 1971; 34:920–936. [PubMed: 4999593]

Schiller PH, Stryker M, Cynader M, Berman N. Response characteristics of single cells in the monkey superior colliculus following ablation or cooling of visual cortex. J Neurophysiol. 1974; 37:181–194. [PubMed: 4204566]

Sherman SM. Thalamocortical interactions. Curr Opin Neurobiol. 2012; 22:575–579. [PubMed: 22498715]

Triplett JW, Owens MT, Yamada J, Lemke G, Cang J, Stryker MP, Feldheim DA. Retinal input instructs alignment of visual topographic maps. Cell. 2009; 139:175–185. [PubMed: 19804762]

Vaiceliunaite A, Erisken S, Franzen F, Katzner S, Busse L. Spatial integration in mouse primary visual cortex. J Neurophysiol. 2013; 110:964–972. [PubMed: 23719206]

Wallace DJ, Greenberg DS, Sawinski J, Rulla S, Notaro G, Kerr JN. Rats maintain an overhead binocular field at the expense of constant fusion. Nature. 2013; 498:65–69. [PubMed: 23708965]

Wang L, Sarnaik R, Rangarajan K, Liu X, Cang J. Visual receptive field properties of neurons in the superficial superior colliculus of the mouse. J Neurosci. 2010; 30:16573–16584. [PubMed: 21147997]

Wang Q, Burkhalter A. Stream-related preferences of inputs to the superior colliculus from areas of dorsal and ventral streams of mouse visual cortex. J Neurosci. 2013; 33:1696–1705. [PubMed: 23345242]

Wickelgren BG, Sterling P. Influence of visual cortex on receptive fields in the superior colliculus of the cat. J Neurophysiol. 1969; 32:16–23. [PubMed: 5765228]

Winkowski DE, Knudsen EI. Top-down control of multimodal sensitivity in the barn owl optic tectum. J Neurosci. 2007; 27:13279–13291. [PubMed: 18045922]

Winkowski DE, Knudsen EI. Distinct mechanisms for top-down control of neural gain and sensitivity in the owl optic tectum. Neuron. 2008; 60:698–708. [PubMed: 19038225]

Wu LQ, Niu YQ, Yang J, Wang SR. Tectal neurons signal impending collision of looming objects in the pigeon. Eur J Neurosci. 2005; 22:2325–2331. [PubMed: 16262670]

Xu NL, Harnett MT, Williams SR, Huber D, O'Connor DH, Svoboda K, Magee JC. Nonlinear dendritic integration of sensory and motor input during an active sensing task. Nature. 2013; 492:247–251. [PubMed: 23143335]

Yilmaz M, Meister M. Rapid innate defensive responses of mice to looming visual stimuli. Curr Biol. 2013; 23:2011–2015. [PubMed: 24120636]

Zhao X, Liu M, Cang J. Sublinear binocular integration preserves orientation selectivity in mouse visual cortex. Nat Commun. 2013; 4:2088. [PubMed: 23800837]

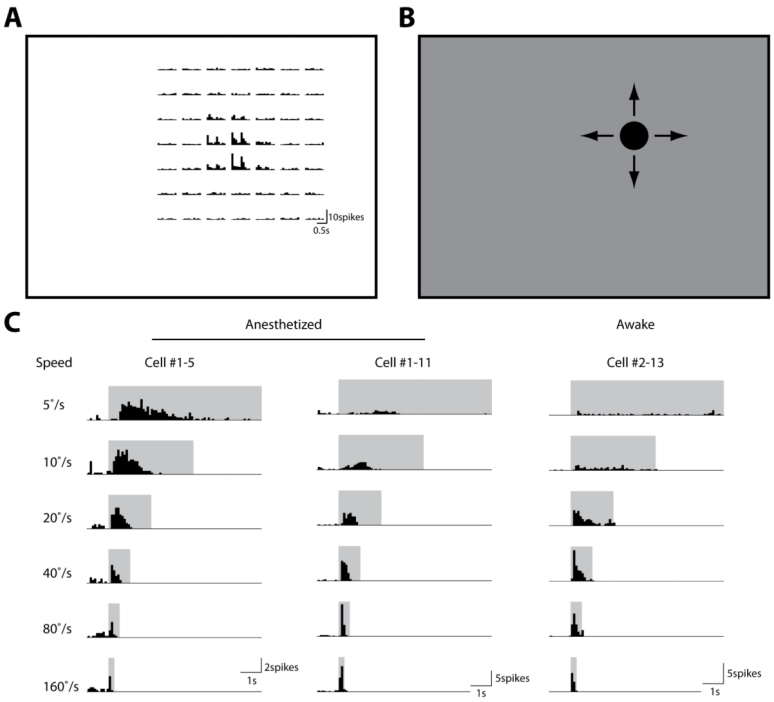

Figure 1. Neuronal responses to looming stimuli in the mouse superior colliculus

(A) Receptive field mapping of an example cell. Small squares (5°×5°) were flashed On and Off at different locations on the stimulus monitor (represented by rectangle). The peristimulus timing histograms of the evoked spikes were shown for corresponding stimulus locations (bin width: 100ms). **(B)** Looming circles were presented at the cell's receptive field center. **(C)** Looming-evoked spike histograms of example cells in anesthetized (left and middle) and awake (right) mice (bin width: 100ms). Stimulus durations were marked by the shaded areas. In anesthetized mice, some cells preferred low looming speeds (left), while most preferred high speeds (middle). Almost all cells preferred high speeds in awake mice (right).

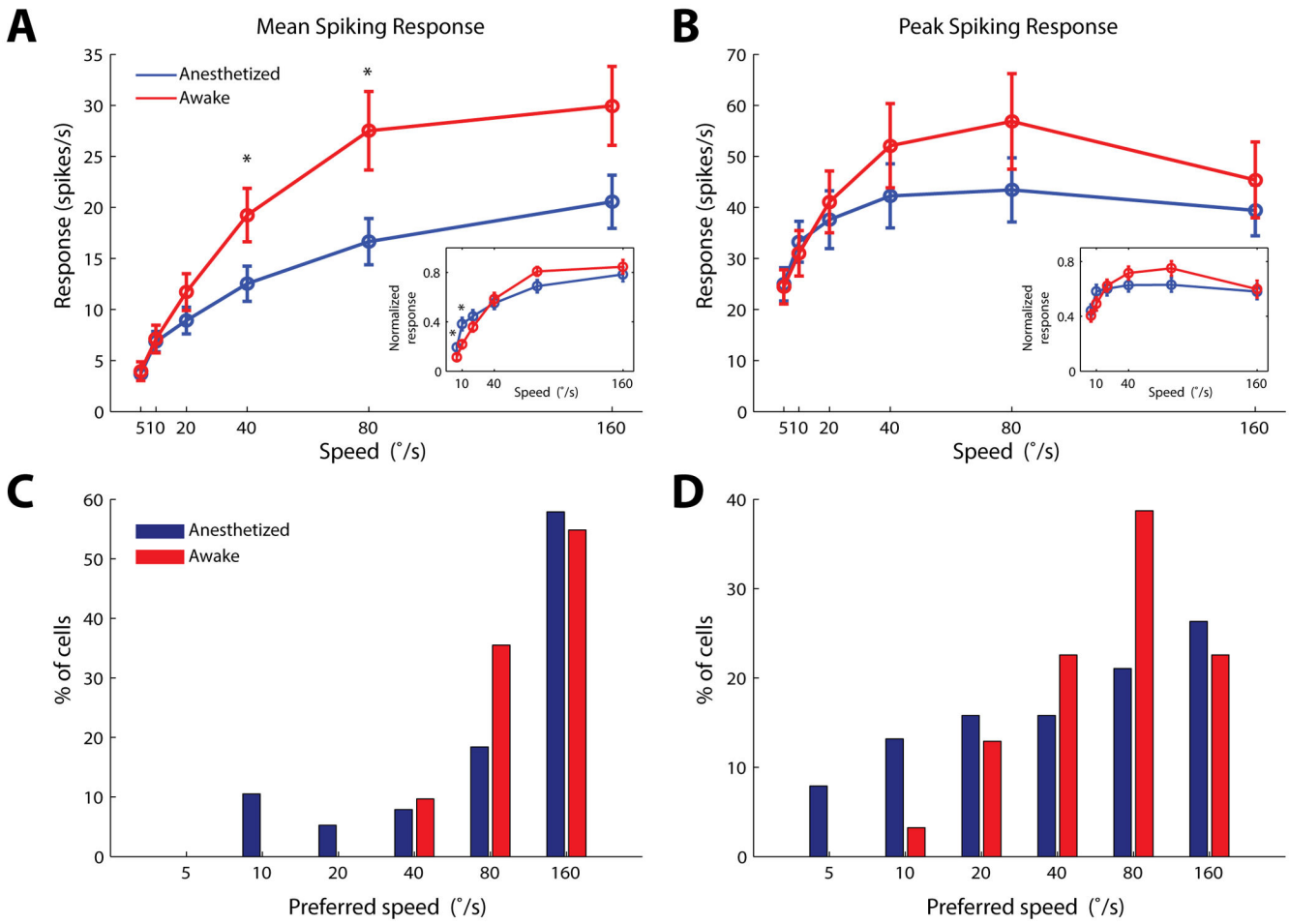

Figure 2. Speed selectivity of SC cells to looming stimuli

(A–B) Population response of SC cells in anesthetized (n=38 cells, 13 mice, blue) and awake (n=31, 12 mice, red) mice, quantified by either mean (**A**) or peak (**B**) responses. Responses in the awake SC were systematically higher than that in the anesthetized condition. The difference is statistically significant ($p<0.05$, Mann-Whitney test) for mean responses at speeds of 40 and 80°/s (**A**). ***Insets***: Normalized SC responses. The response of each cell was first normalized by the response to its preferred speed. Normalized responses were then averaged across the population. The normalized tuning curves were moderately skewed toward higher speeds in awake animals ($p<0.05$, Mann-Whitney test, for speeds of 5 and 10°/s in the inset of **A**). **(C–D)** Distributions of the preferred speed for individual neurons, analyzed by mean (**C**) or peak (**D**) responses. The distribution quantified by peak responses was moderately right shifted in awake mice ($p=0.06$, χ^2 test). Pooled data were presented as mean ± S.E.M.

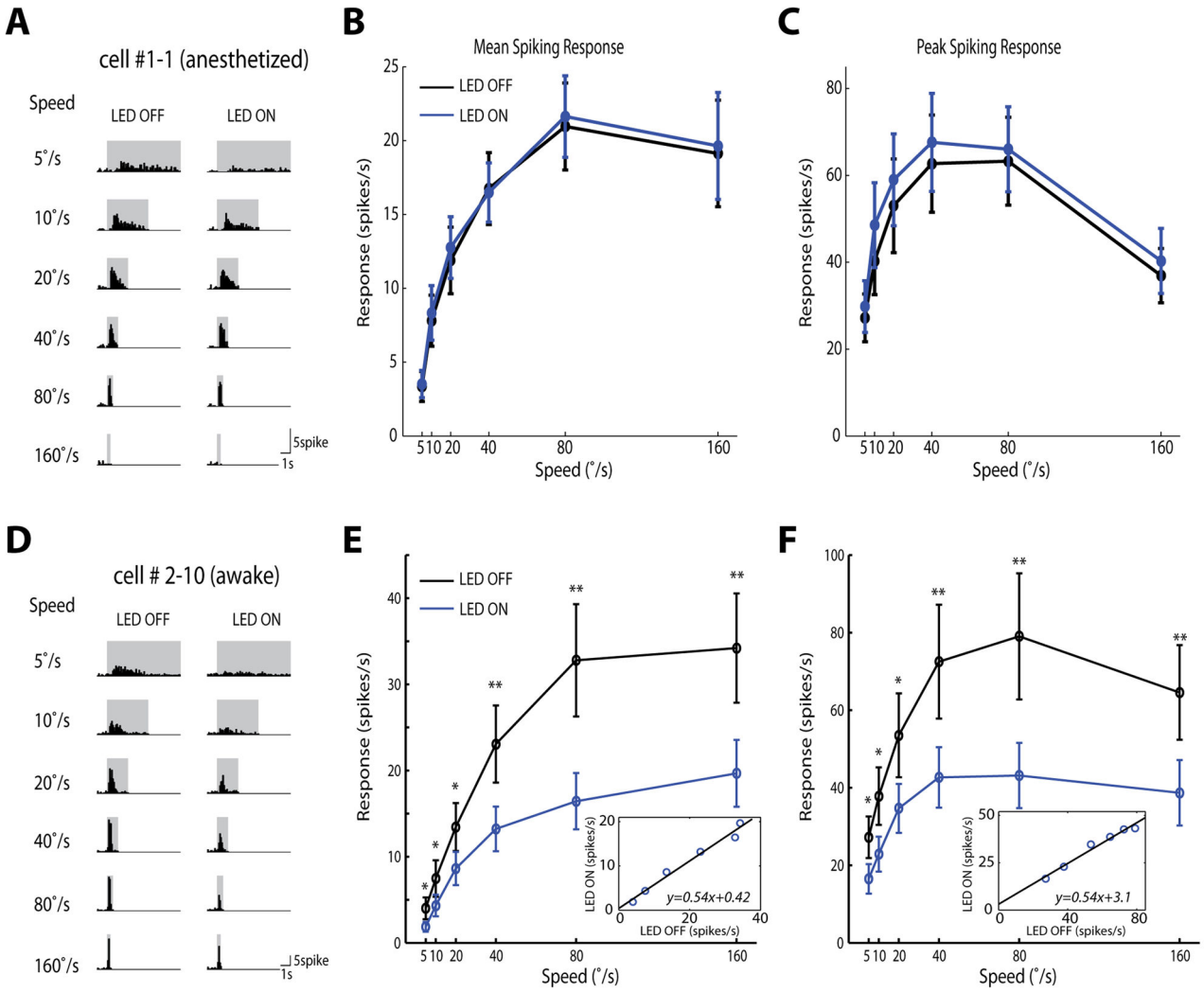

Figure 3. Silencing visual cortex reduces the gain of looming-evoked responses in the SC in awake mice

(A) Spike histogram of an example SC cell in anesthetized mice, with the LED light OFF for the control and LED ON for silencing cortex (bin width: 100ms). Changes were barely seen at any speed. **(B–C)** Silencing cortex (blue) did not alter mean (**B**) or peak (**C**) responses in anesthetized mice, compared to the control condition (black) (n=18 cells, 6 mice). **(D–F)** Same plots as in **A–C**, but in awake mice. Silencing cortex significantly reduced mean and peak responses of SC cells across all tested stimulus speeds (*: p<0.05, **: p<0.01, paired t-test, n=15 cells, 6 mice). ***Insets***: Linear transformation of responses between the LED ON and OFF conditions. Pooled data were presented as mean±S.E.M.

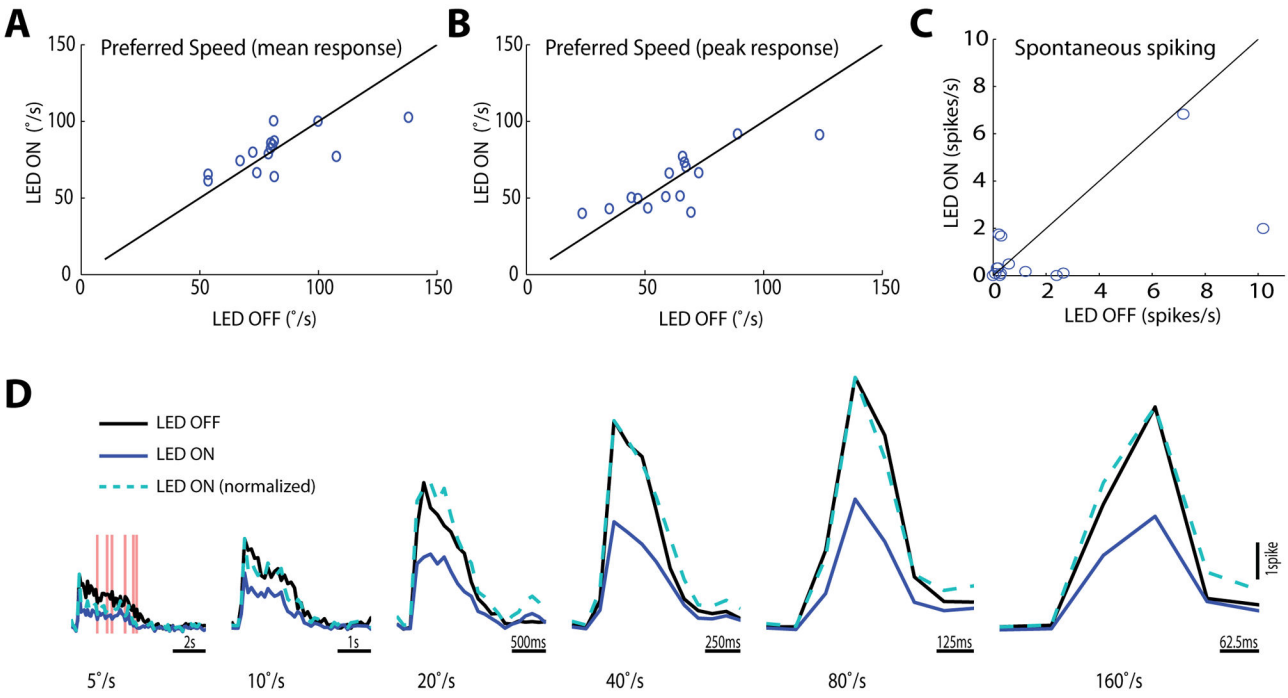

Figure 4. Silencing visual cortex does not alter SC speed tuning or time course in response to looming in awake mice

(A–B) Preferred speed analyzed by the mean (**A**) and peak (**B**) spiking rate, respectively. S_{pref}–weighted was calculated as described in Experimental Procedures. No significant alteration of the preferred speed was seen (p=0.77 in A and 0.56 in B, n=15, paired t-test). **(C)** Spontaneous spiking rates of SC cells before and after silencing cortex. A trend of slight reduction was seen, but not statistically significant in our dataset (p=0.21, n=15, paired t-test). The spontaneous spiking rates were 1.7±0.9spikes/s for control condition, and 0.8±0.5spikes/s when cortex was silenced (mean±S.E.M.). **(D)** Instantaneous spiking rate in the awake SC, averaged across all cells (bin width of 100ms; n = 15; black for the control, blue for silencing cortex, and light blue dashed lines for normalized blue curves to the control's peak). The control and the peak-normalized responses after silencing cortex were only significantly different at the late phase of the lowest speed, as marked by pink shades ($p<0.05$, paired t-test). Note that responses to stimuli with different speeds were plotted with different time scales.

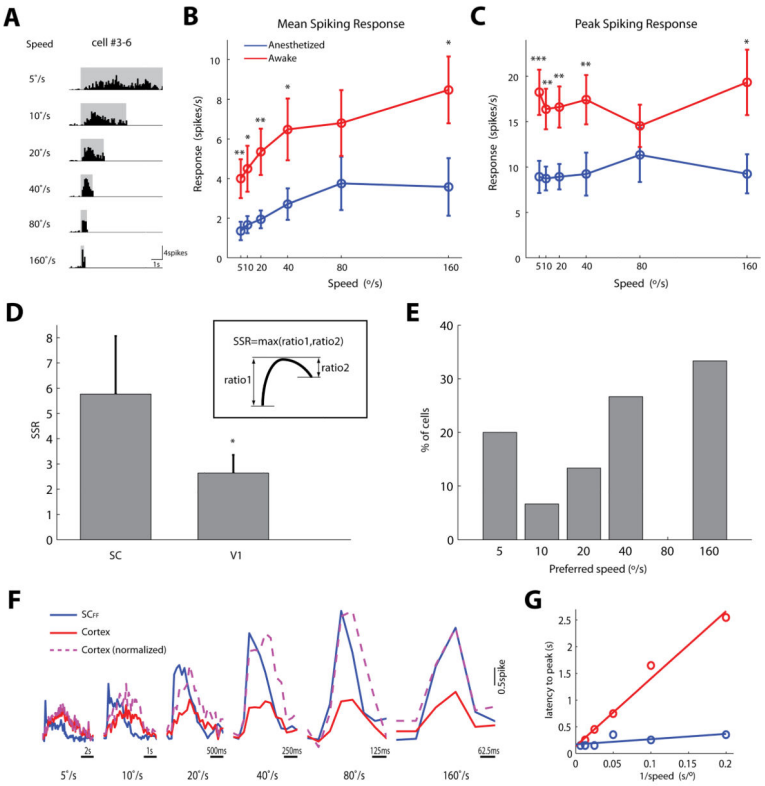

Figure 5. Responses of V1 layer 5 cells to looming stimuli

(A) Spike histogram of an example V1 layer 5 cell in awake mice. **(B–C)** Mean (**B**) and peak (**C**) responses of layer 5 cells in anesthetized (blue) and awake (red) animals. Unlike SC cells, cortical cells were poorly tuned to looming speed under both conditions. The responsiveness was significantly higher in awake animals (*: $p<0.05$, **: $p<0.01$, ***: $p<0.001$; Mann-Whitney test, n=18 cells from 7 anesthetized and 15 cells for 7 awake mice). **(D)** Speed selectivity ratio (SSR) of individual cells is much higher in the SC than in V1, both recorded in awake animals ($p<0.05$, Mann-Whitney test, n=21 for SC and 15 for cortex). **Inset**: Calculation of SSR (see Supplemental Experimental Procedures for details). **(E)** Distribution of the preferred speed of individual V1 neurons. Peak responses were used for quantifications in both **D** and **E. (F)** Instantaneous spiking rates in the SC and V1 in awake mice, averaged across all cells (bin width of 100ms; n = 15 for both SC and V1). The blue curves are for the SC responses when cortex was silenced (SC_{FF}), red for V1 responses, and purple dashed lines for V1 responses normalized to the peak of SC_{FF}. **(G)** The latencies of peak responses plotted against the inverse of the looming speed. Straight lines were fitted by linear regression. The slope was 12.6 for V1 (blue) and 1.0 for the SC_{FF} (red). Pooled data were presented as mean±S.E.M.

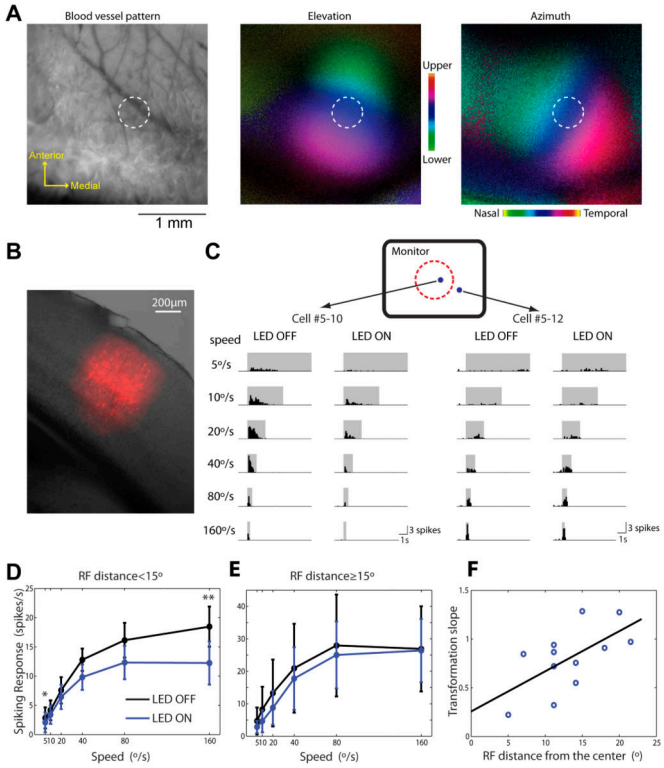

Figure 6. The effect of corticotectal projection is retinotopically organized

(A) Intrinsic imaging of cortical retinotopic maps for guiding viral injection. Left panel: cortical blood vessel pattern used as landmarks. Middle and right: elevation and azimuth maps in V1. Positions in the visual space were color coded as shown in the color scale. In both cases, the range (from green to red) spanned ~60° in visual space. The brightness of each pixel represented the response magnitude. White dashed circles marked the estimated expression area, ~450μm in diameter. **(B)** A coronal section of the injection site in V1. Overlaid bright-field image and red fluorescence signals. **(C)** Spike histograms of example SC cells in response to looming in the absence and presence of optogenetic stimulation. Blue dots in the top diagram marked their receptive field centers on the monitor. The dotted red circle marked a 15° radius circle around the monitor's center. **(D)** Mean looming-evoked responses of SC cells that had receptive field centers inside the circle. Silencing cortex significantly reduced their visual responses (n=8, $p<0.05$ for 5°/s, $p<0.01$ for 160°/s, paired t-test). **(E)** Mean responses of SC cells with receptive field centers outside the circle. Silencing cortex had no effect on their visual responses (n=4, $p>0.3$ for all speeds, paired t-test). **(F)** Significant correlation between the transformation slope and receptive field distance from the monitor's center (n=12 cells, 6 mice, correlation coefficient=0.62, $p<0.05$). Black line marked the linear regression of the data points. The transformation slope is the slope of the linear regression of mean responses between LED ON and OFF conditions for each cell. Pooled data were presented as mean±S.E.M.